University of Sistan and Baluchestan

Challenges in Nano and Micro Scale Science and Technology

Online ISSN: 2821 - 000X

# The Application of Photocatalytic Degradation Process in The Removal of Methyl Orange Dye Using Magnetic Nanocomposite from Aqueous Solutions

**Sanaz Khammar[1]✉ | Arash Khoshnoodfar[2]**

1. Campus of Science and Technology, University of Sistan and Baluchestan, Zahedan, Iran. Email: Sanaz_khammar@yahoo.com
2. Department of Environmental Engineering, Faculty of Natural Resources and Environment, University of Birjand, Birjand, Iran.

**Article Info**

**Article type:**
Research Article

**Keywords**:
Core-shell nanocomposite, methyl orange dye, photocatalytic degradation, optimization of surface response method

**ABSTRACT**

This research focuses on the removal of the dye methyl orange from aqueous solutions, a common environmental pollutant found in textile and dyeing industries. For this purpose, the efficiency of the photocatalytic degradation process using $Fe_2O_3$@ZnO core-shell nanocomposite was investigated in order to remove dye pollutant methyl orange from aqueous solutions using the response surface method (RSM) in the central composite design (CCD). Scanning electron microscopic (SEM), X-ray diffraction (XRD) and X-ray energy diffraction (EDX) analyzes were used to investigate the structural characteristics of the synthesized nanocomposite. Then, in order to investigate the efficiency of the synthesized nano photocatalyst in the process of photocatalytic degradation, the effect of important functional variables such as photocatalyst dose, pH, temperature and time were investigated to optimize the maximum dye removal. Based on the statistical results, the optimal efficiency of dye removal was 49.80% with a catalyst dose of 3 g/L, pH = 4, temperature 44.12 °C and irradiation time 148.34 min. Among the investigated parameters, temperature and pH had a significant effect on the photocatalytic degradation process. Also, the recovery of $Fe_2O_3$@ZnO photocatalyst during five consecutive cycles showed that the synthesized nanocomposite has good recovery capability for removing methyl orange from aqueous solutions. The experimental results indicate that the use of $Fe_2O_3$@ZnO nanoparticles has a high efficiency in removing dye pollutants and can also be an ideal method for treating dye-polluted wastewater, due to their excellent selective absorption and good recovery.

## INTRODUCTION

Dye pollution has been a significant environmental concern due to the extensive use of dyes in various industries, including textiles, printing, food production, and the manufacturing of dye raw materials (Islam et al., 2023). With an estimated annual production of 700,000 to 1,000,000 tons of dyes, it is alarming that approximately 17-20% of these dyes are discharged into the environment during production processes (Rahman, 2020). The toxic and carcinogenic properties of many dyes pose serious threats to human health and ecosystems, necessitating urgent research into effective treatment methods for contaminated water (Alsukaibi, 2022). Historically, the textile industry has been a major contributor to dye pollution, with azodyes accounting for about 50% of all textile dyes (Slama et al., 2021). This high prevalence highlights the need for the development of efficient and straightforward methods for dye removal from wastewater. Various techniques have been explored to address this challenge, including surface adsorption on natural and synthetic adsorbents, biological processes, electrochemical oxidation, and advanced oxidation processes (AOPs) (Peramune et al., 2022). AOPs have emerged as particularly effective solutions for removing resistant and emerging pollutants. These processes generate highly reactive hydroxyl radicals (OH•), capable of mineralizing complex organic compounds (Ismail and Sakai, 2022). Over the years, different types of AOPs, such as UV oxidation, photocatalysis, and combinations like UV/$H_2O_2$/$O_3$, have been investigated for their efficacy in degrading dye pollutants. As energy costs associated with

**How to Cite this paper**: Khammar S, Khoshnoodfar A. The Application of Photocatalytic Degradation Process in The Removal of Methyl Orange Dye Using Magnetic Nanocomposite from Aqueous Solutions. *Challenges in Nano and Micro Scale Science and Technology*. 2023; 11(1): 31-38. DOI: 10.22111/cnmst.2024.49154.1250

© Khammar S, Khoshnoodfar A.

Publisher: University of Sistan and Baluchestan.

DOI: 10.22111/cnmst.2024.49154.1250

UV lamps remain high, there has been a shift toward utilizing visible light for the purification of drinking water. This transition has led to increased interest in the doping of transition metals on metal oxides, which enhances photocatalytic activity (Giwa et al., 2021).

Doping creates intermediate bands and increases oxygen vacancies, facilitating oxidation and reduction reactions during the photocatalytic process (Gallego-Ramírez et al., 2022). Zinc oxide, recognized for its unique electrical and optical properties, has been extensively studied due to its stability against optical and chemical corrosion and its ability to decompose toxic organic compounds under UV light (Batra et al., 2022). However, its high bandgap of 3.3 eV limits activation under visible light, prompting research into metal doping to reduce the bandgap and improve the generation of electron-hole pairs (Yashni et al., 2021). Recent advancements have focused on creating composites of two or more semiconductors to enhance photocatalytic efficiency. This approach not only increases the number of vacancies and surface defects but also establishes a new bandgap that boosts the optical activity of the catalyst (Sushma and Girish Kumar, 2017). Gupta et al. (2018), in a study, investigated the ability of zinc oxide composite doped with iron, copper and silver in bacterial inactivation under the influence of visible light. The results showed that the composition of zinc oxide doped with iron and copper had a higher ability compared to zinc oxide doped with iron and silver, which was attributed to the higher absorption of visible light by copper oxide (Gupta et al., 2018). In another study, Taufik and Saleh (2017) also investigated dye removal in the presence of visible light, UV light and ultrasound using $Fe_3O_4$/ZnO/CuO catalyst. The results showed that the catalyst with a lower percentage of CuO has more photocatalytic activity in the presence of UV light, while in the presence of visible light, the composite with a higher percentage of CuO had more activity. Ultrasonic combination also increased the decomposition rate and hydroxyl radical and hole were the two dominant species in the decomposition process (Taufik and Saleh, 2017).
The present research in this field aims to provide innovative and sustainable solutions for effective dye removal, addressing the critical issue of water pollution and its impact on environmental health. The novelty of this research lies in its focus on advanced oxidation processes, particularly those utilizing visible light for the degradation of resistant dye pollutants. The integration of transition metal doping into metal oxides, such as zinc oxide, is a cutting-edge approach that enhances photocatalytic activity under visible light. This innovation addresses the limitations of conventional UV-based methods, which often incur high energy costs and are less sustainable. Furthermore, the development of composite materials that optimize electron-hole pair generation while minimizing recombination is a key advancement. By creating new bandgaps through the combination of semiconductors, the research aims to improve the efficiency of photocatalysts in degrading complex organic compounds. The aim of the present study is to investigate the efficiency of the photocatalytic process in the decomposition of the dye pollutant methyl orange using the $Fe_2O_3$@ZnO catalyst and to examine important functional variables such as photocatalyst dose, pH, temperature and time in order to optimize the maximum decomposition of methyl orange.

## MATERIALS AND METHODS

### Synthesis of $Fe_2O_3$@ZnO photocatalyst

For the synthesis of $Fe_2O_3$@ZnO catalyst, the sol-gel combustion method was used. The foundation of this method lies in the simultaneous deposition of two or more compounds. In this method, for the synthesis of pure zinc oxide, the precursor zinc acetate dihydrate ($Zn(CH_3COO)_2.2H_2O$) was dissolved in an alkaline medium with a suitable pH and by applying energy to the system, white ZnO powder particles were synthesized. For this purpose, 3 grams of zinc acetate was dissolved in 16 mL of distilled water and 0.387 grams of $Fe(NO_3)_3.9H_2O$ was added to it and the pH of the solution was neutralized using ammonia. The resulting solution was poured into a 100 mL beaker and mixed for 3 hours at a temperature of 80 °C. Then it was heated on a heater for another 10 hours at a temperature of 210 °C to dry. The sediment obtained was transferred to the porcelain crucible to be completely calcined at 500°C for 3 hours and the $Fe_2O_3$@ZnO catalyst was made (Shekoohiyan et al., 2020).

### Photocatalytic reactor for dye removal

This process was carried out in a photoreactor made of glass with a volume of 300 mL, an internal diameter of 80 mm and a height of 150 mm, in the center of which a quartz protector was installed to place the D1S xenon lamp (12V, 35W) (Cutoff UV filter was used to remove wavelengths less than 400 nm). In order to protect the reactor from ambient light interference, the photoreactor was covered with aluminum foil. This process was continuously operated and the effect of parameters such as photocatalyst dose (1-4 g/L), pH (4-9), temperature (15-50 °C) and time (210-40 min) was investigated. For each step, a certain amount of photocatalysts was added separately to dye solutions with a certain initial concentration in a certain volume of the solution with the desired pH and stirred for 20 min in a dark place; The purpose of this work is to balance the amount of absorption of dye molecules by the catalyst, so that the effect of molecular degradation of the photocatalyst on the removal of dye pollutants can be investigated more precisely. After this period, 2 mL of the solution was sampled to determine the concentration of the dye substance in the environment after the absorption process with the help of UV-visible analysis. Finally, the dye removal percentage was calculated from the following equation (1):

$$Removal\ \% = \frac{C_0 - C_i}{C_0} \times 100 \quad (1)$$

$C_0$ and $C_i$ are the initial concentration and final concentration of the dye, respectively.

### Response surface methodology (RSM)

Design generation, regression and graphical analyses were performed by Design-Expert software 7.0 (DOE, Stat-Ease

Inc., Minneapolis, MN, USA) for experimental data processing to attain the optimal photocatalytic degradation efficiency of methyl orange dye from aqueous solutions by synthesized nano photocatalyst. The central composite design (CCD) under response surface methodology (RSM) was employed to plan the experiments and identify the interaction effects of the four independent variables and the significance of factors to design the experimental runs (Khammar et al., 2020a; Soleimani et al., 2023). Actually, RSM, as a strong design technology based on the CCD, could examine the effect of multiple factors and their interactions on one or more response variables simultaneously, and also could be employed in the optimizing processes (Khammar et al., 2020b). The design of the experiments based on the CCD is also given in Table 1, which was affected by the variables, pH (A), catalyst dose (B), reaction time (C) and temperature (D) in the experiments, which results Experiments were calculated and coded using design software.

## RESULTS AND DISCUSSIONS

The characteristics of the crystal structure of the synthesized catalysts and their crystallite size were investigated using X-ray diffraction analysis and the result is shown in Figure 1. As shown in Fig. 1, the ZnO catalyst has peakbasis of s at (100), (200), (101), (102), (103), (110) and (112) angles, which are coded card (JCPDS No. 79-0206) which is related to ZnO is in compliance. Iron oxide also formed a peak at 2Θ equal to 35.7 degrees and angle (311) in the $Fe_2O_3$@ZnO catalyst, which is compatible with the card code (JCPDS No. 1346-39) related to iron oxide. The crystallite size of synthesized ZnO and $Fe_2O_3$@ZnO catalysts was found to be 345 and 205 nm, respectively, using the Scherrer-Debye equation. In order to investigate the morphology and elemental composition of the $Fe_2O_3$@ZnO catalyst, SEM and EDX analyzes were performed, the results of which are shown in Fig. 2 and Fig. 3. SEM images show that the synthesized catalyst was spherical and the size of $Fe_2O_3$@ZnO particles is smaller compared to ZnO, and the SEM and XRD results are in agreement. The elemental analysis with EDX on the $Fe_2O_3$@ZnO catalyst, the results of which are presented in Fig. 2, showed that oxygen, iron and zinc elements can be seen in the chart, which indicates the absence of contamination and the purity of the catalyst. Also, the weight percentage of zinc, iron and oxygen elements were 90.4, 8.5 and 1.1%, respectively.

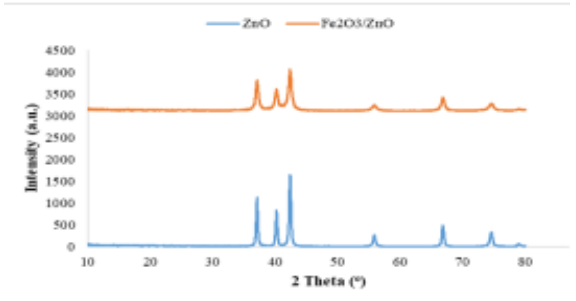



**Fig. 1.** X-ray diffraction analysis of ZnO and $Fe_2O_3$@ZnO catalysts

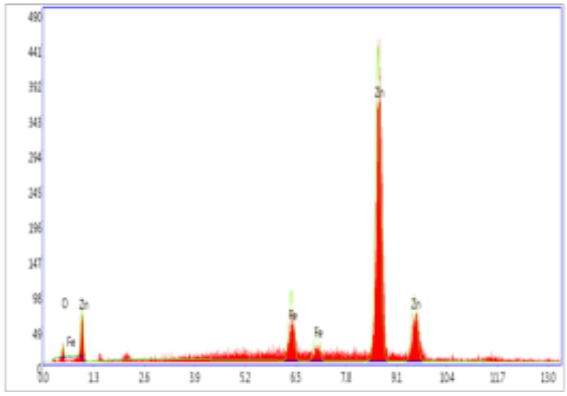


**Fig. 2.** Elemental analysis of $Fe_2O_3$@ZnO catalyst

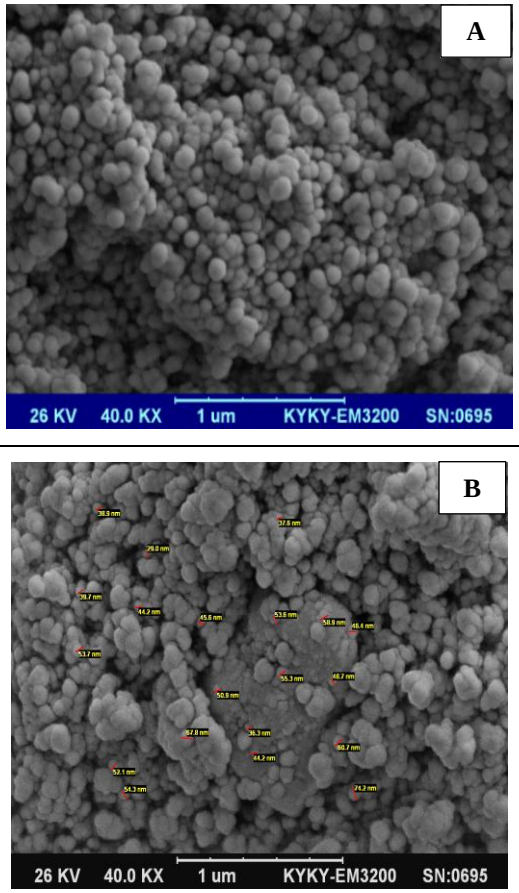



**Fig. 3.** SEM images of ZnO and $Fe_2O_3$@ZnO catalysts

The percentage of methyl orange dye removal in different experiments was calculated using formula 1 and the relationship between the four variables of photocatalyst dose, pH, temperature and time, with the percentage of methyl orange dye removal was analyzed using the response surface method (RSM). According to CCD-RSM, a total number of 30 experimental runs were conducted based on variables and the responses of 16 factorial points, 8 axial points and 4 center points and 3 replicates were employed as presented in Table 1.

**Table 1**
Experimental Design matrix and results

| Run | Real (coded) values | | | |
|---|---|---|---|---|
| | A | B | C | D |
| 1 | 4/03(-1) | 1(-1) | 43/68(-1) | 15/86(-1) |
| 2 | 8/97(+1) | 1(-1) | 43/68(-1) | 15/86(-1) |
| 3 | 4/03(-1) | 3(+1) | 43/68(-1) | 15/86(-1) |
| 4 | 8/97(+1) | 3(+1) | 43/68(-1) | 15/86(-1) |
| 5 | 4/03(-1) | 1(-1) | 206/32(+) | 15/86(-1) |
| 6 | 8/97(+1) | 1(-1) | 206/32(+) | 15/86(-1) |
| 7 | 4/03(-1) | 3(+1) | 206/32(+) | 15/86(-1) |
| 8 | 8/97(+1) | 3(+1) | 206/32(+) | 15/86(-1) |
| 9 | 4/03(-1) | 1(-1) | 43/68(-1) | 44/14(+1) |
| 10 | 8/97(+1) | 1(-1) | 43/68(-1) | 44/14(+1) |
| 11 | 4/03(-1) | 3(+1) | 43/68(-1) | 44/14(+1) |
| 12 | 8/97(+1) | 3(+1) | 43/68(-1) | 44/14(+1) |
| 13 | 4/03(-1) | 1(-1) | 206/32(+) | 44/14(+1) |
| 14 | 8/97(+1) | 1(-1) | 206/32(+) | 44/14(+1) |
| 15 | 4/03(-1) | 3(+1) | 206/32(+) | 44/14(+1) |
| 16 | 8/97(+1) | 3(+1) | 206/32(+) | 44/14(+1) |
| 17 | 3(-α) | 2(0) | 125(0) | 30(0) |
| 18 | 10(+α) | 2(0) | 125(0) | 30(0) |
| 19 | 6/5(0) | 0/5(-α) | 125(0) | 30(0) |
| 20 | 6/5(0) | 3/5(+1) | 125(0) | 30(0) |
| 21 | 6/5(0) | 2(0) | 10(-α) | 30(0) |
| 22 | 6/5(0) | 2(0) | 240(+α) | 30(0) |
| 23 | 6/5(0) | 2(0) | 125(0) | 10(-α) |
| 24 | 6/5(0) | 2(0) | 125(0) | 50(+α) |
| 25 | 6/5(0) | 2(0) | 125(0) | 30(0) |
| 26 | 6/5(0) | 2(0) | 125(0) | 30(0) |
| 27 | 6/5(0) | 2(0) | 125(0) | 30(0) |
| 28 | 6/5(0) | 2(0) | 125(0) | 30(0) |
| 29 | 6/5(0) | 2(0) | 125(0) | 30(0) |
| 30 | 6/5(0) | 2(0) | 125(0) | 30(0) |

The predicted values were obtained using Design-Expert software and model fitting technique, which are in good agreement with the obtained experimental data. Response surface method (RSM) and ANOVA analysis of variance were used for the model and the results for the dependent variable are summarized in Table 2. Finally, the significance and influence of each independent variable were determined using F-values and the accuracy of the results with prob > F. In this study, the variance analysis of the data showed that the effects of the main variables of photocatalyst dose, temperature, time and initial pH, the squared effects of temperature, time, photocatalyst dose, initial pH, the interaction between pH factors and photocatalyst dose, pH and time, pH and temperature, photocatalyst dose and time, photocatalyst dose and temperature, time and temperature are significant in the model ($p<0.05$). The F-value of the model for the percentage of dye removal in the photocatalytic process was 852.29 and the value of prob > F was less than 0.0001 for the dependent variables mentioned in the model, which indicates the significance of the model and the results obtained (prob value > F less than 0.05 indicates that the model is statistically significant). Therefore, according to the coefficients and P-value and F-value, the obtained regression model is significant and reliable. The results of the analysis of variance showed that the values of the lack of fit of the model (P-value < 0.05) were not significant, which indicates that the obtained model is valid and statistically reliable for the desired dependent variable. A summary review of the model outputs determined that the model is statistically significant for the dependent variable and therefore can be used for further analysis (Amini and Younesi, 2009). Correlation for the dependent variable was calculated as regression square ($R^2$). In the present study, the determined value of this coefficient for the dependent variable was 0.9831, indicating that the regression equations are statistically significant. This suggests that less than 0.2% of the total analysis of variance is not significant and cannot be explained by the model. Determining the predicted value of the regression coefficient = 0.8962 Pred.$R^2$ has a logical and acceptable relationship with the experimental value determined for the coefficient Adj = 0.9634. is $R^2$. The predicted and adjusted regression coefficient in this modeling is very high and shows that the model is very consistent with the results of the experiments and can well predict the desired response (percentage of dye removal). Parallel to these results, the relatively low value of the coefficient of variance (CV) of 3.05% for the dependent variables indicates the accuracy of the measurements and the reliability of the tests performed. The goodness of fit of the model was evaluated using analysis of variance. The low values of SD and PRESS, which were 1.10 and 90.02, respectively, indicate the superiority of the fitted models on the experimental data. According to the regression equation, the significant variables include (from the most significant to the least significant), pH effect > pH squared effect > temperature squared effect > model > temperature squared effect.

**Table 2**
Analysis of variance (ANOVA) results for model terms.

| Response | Source | df | Square | F value | prob > F |
|---|---|---|---|---|---|
| Removal of methyl orange | Model | 852.29 | 60.88 | 49.89 | <0.0001 |
| | Residual | 14.64 | 1.22 | | |
| | Lack of Fit | 11.97 | 1.71 | 3.20 | 0.1097 |
| | Pure Error | 2.67 | 0.53 | | |
| | Total | 866.93 | | | |

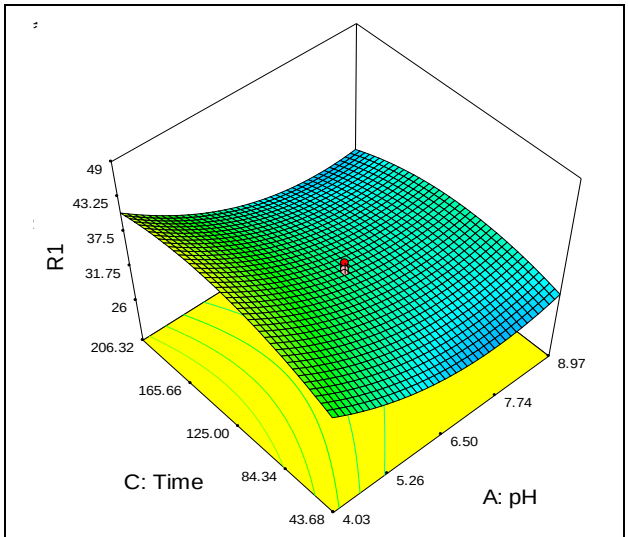
The first multiple regression coefficients of the dye removal model by photocatalytic method are shown in Table 3. According to p-value, all independent variables in

this study (A, B, C, D, AB, AC, AD, BC, CD, $A^2$, $B^2$, $C^2$ and $D^2$) were significant.

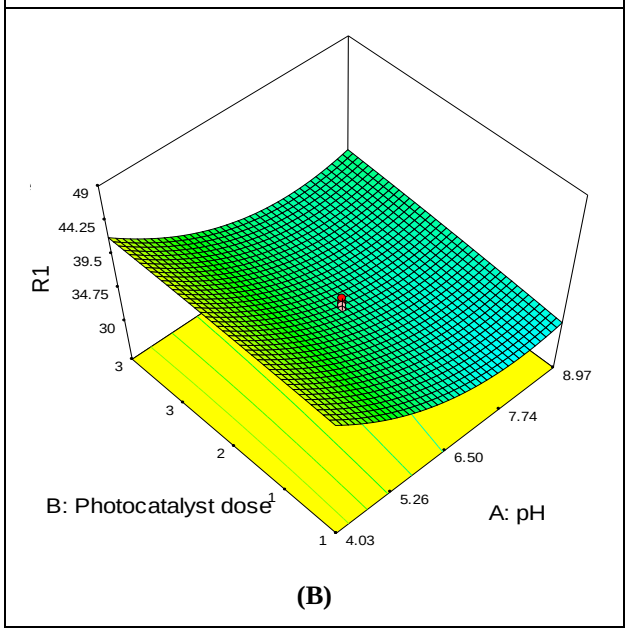
**Table 3**
Multiple regression coefficients of the model

| Source | F value | prob > F |
|---|---|---|
| A- pH | 279.19 | <0.0001 |
| B-Photocatalyst | 9.52 | 0.0094 |
| C-Time | 5.75 | 0.0336 |
| D-Temperature | 17.23 | 0.0013 |
| AC | 17.64 | 0.0012 |
| BD | 19.76 | 0.0008 |
| CD | 26.86 | 0.0002 |
| $A^2$ | 127.50 | <0.0001 |
| $C^2$ | 46.03 | <0.0001 |
| $D^2$ | 100.81 | <0.0001 |

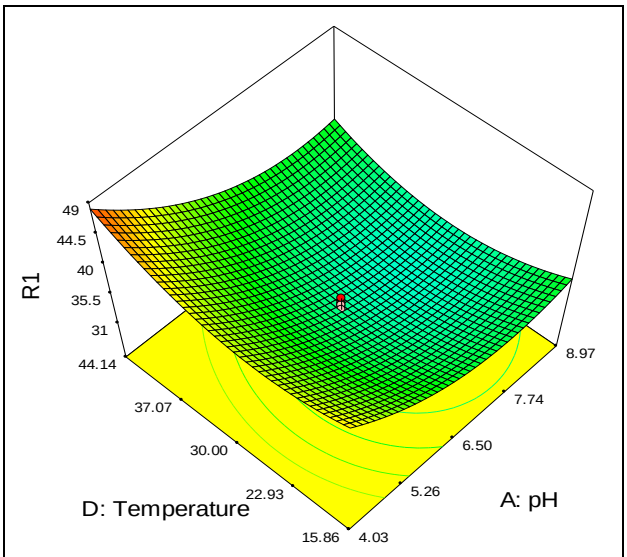
Fig. 4 (a-f) shows the effect of photocatalyst dose, time, temperature and pH on the removal of methyl orange dye from aqueous solutions in the photocatalytic process.



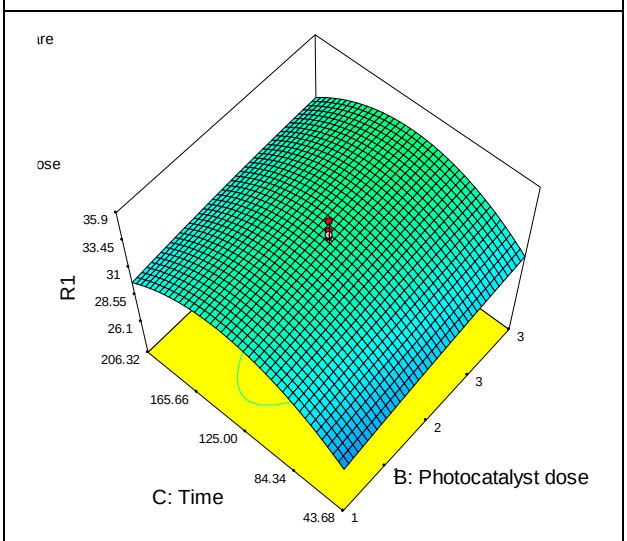

**(A)**



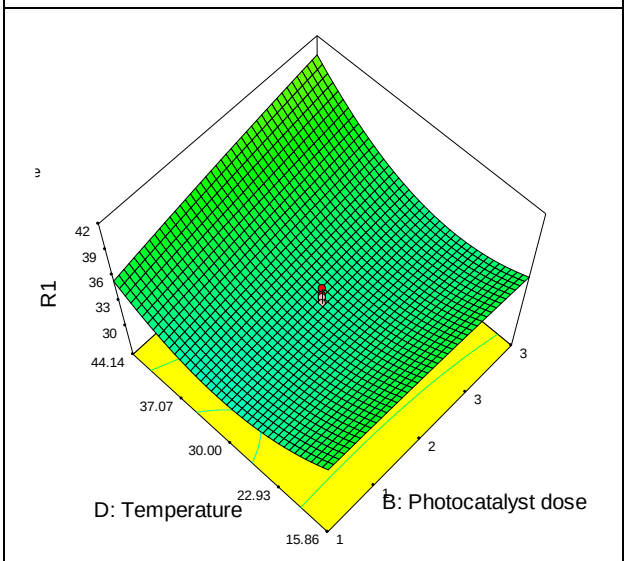

**(B)**




**(C)**




**(D)**




**(E)**

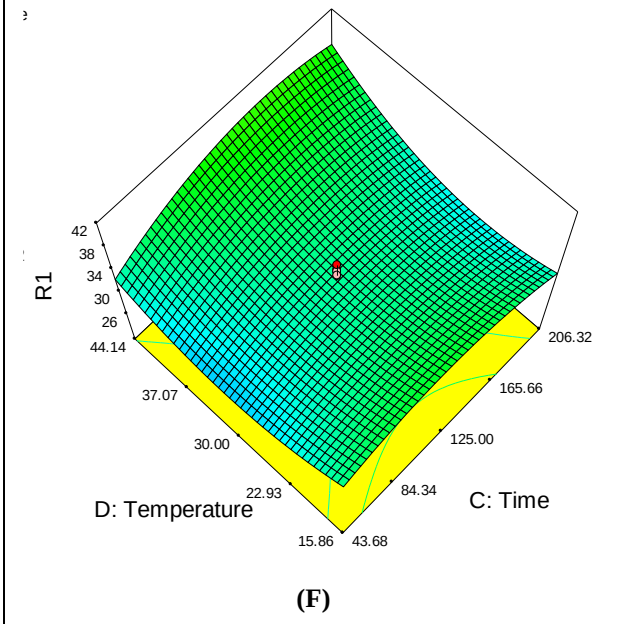



**Fig. 4.** The effect of photocatalyst dose, time, temperature and pH on the removal of methyl orange dye in the photocatalytic process

Fig. 4 shows the effect of photocatalyst dose, time, temperature and pH on the amount of methyl orange dye removal in the photocatalytic process. The effect of time and pH on the percentage of dye removal is shown in Fig. 4(a). In this graph, the pH value varied between 4.03 and 8.79 and the time between 43.68 and 206.32 min. The maximum removal efficiency was obtained at acidic pH, which is due to the better performance of OH·radicals in acidic environments (Song et al., 2010). Since the rate of dye oxidation occurs at pH between 3 and 5, and oxidation decreases at higher pH. This behavior is due to the property of the catalyst, which is strongly dependent on the presence of $H^+$ ions. At pH higher than 7, the catalyst surface becomes negative and causes the absorption of OH ions. In addition, the formation of HO· radicals hinders the conduction of the band where dissolved oxygen molecules have changed to $O^-_2$. But this reaction with $H^+$ ions happens less because its concentration is low. Therefore, pH strongly affects the formation of ·OH and $HO^-_2$ radicals (Preočanin and Kallay, 2006). In similar studies, Yigit et al. (2009) and Cho et al. (2002) reported that reducing pH from 9 to 3 significantly increased the removal efficiency of organic compounds. Fig. 4 (b) shows the simultaneous effect of photocatalyst dose and pH. In this diagram, the photocatalyst dose values ranged from 0.94 to 3.6 g/l and pH ranged from 4.03 to 8.97. In this graph, according to graph 4 (a), the dye removal efficiency increased with the decrease in pH, and also with the increase of the photocatalyst dose, the efficiency of the process also increased, so that the dye removal increased from 30.40% at the dose of 0.94g/liter of photocatalyst and 8.97%. pH = reached 42.25% of dye removal in photocatalyst dose of 3.06 g/l and pH = 4.03. Increasing the dose of photocatalyst increases the active sites available for absorption. However, increasing the dose of photocatalyst more than a certain limit does not cause a significant change in the efficiency of the photocatalytic degradation process (Al-Sayyed et al., 1991). This happens when the maximum amount of absorption of photons in the reactor is achieved. Several studies have reported a decrease in degradation efficiency with increasing photocatalyst dosage above a certain limit (Al-Sayyed et al., 1991; Wang et al., 1999). Other factors related to this reduction are the prevention of light penetration and light scattering (Gaya et al., 2010). This reduces the available active sites and prevents the formation of electron-hole pairs. Also, in the photocatalyst suspension at a high dose, accumulation and clumping of photocatalysts occur, which reduces the available active sites and subsequently the efficiency of the system (Gaya et al., 2010). Fig. 4(c) shows the simultaneous effect of pH and temperature on the dye removal efficiency. In this graph, the pH ranged from 4.03 to 8.97. In this graph, as in Figure 4(b) and 4(a), the dye removal efficiency increased with decreasing pH and increasing temperature, so that dye removal increased from 31.76% at pH = 8.97 and temperature = 15.86 °C dye removal was reached 48.15 %at pH=4.03 and temperature at 44.14 °C. According to the obtained results, increasing the temperature increases the electron transfer of the valence band of ZnO to higher energy levels and facilitates the production of electron-holes, which are used for primary oxidation and reduction reactions (Gaya et al., 2010). Holes ($hv_{b+}$), electrons ($e_{cb}$) and hydroxyl radicals ($HO^{\cdot}$) produced as a result of UV light radiation cause the destruction and decomposition of organic pollutants into intermediate compounds, and then the intermediate compounds are decomposed into $CO_2$ and $H_2O$. Zeltner et al. (1993) showed that increasing the reaction temperature increases the speed of all reactions except the formation of electron-hole pairs in the system (Zeltner Jr, 1993). In other words, increasing the reaction temperature reduces the solubility of oxygen in the effluent. Decreasing the dissolved oxygen concentration decreases the rate of electron withdrawal from the photocatalyst surface. The study conducted by Fox and et al. (1994) on aliphatic alkali compounds showed that the photocatalytic degradation of aliphatic compounds is sensitive to temperature changes and increases with increasing temperature (Fox et al., 1994). Hofstadler et al. (1994) investigated the effect of temperature on the photocatalytic degradation of 4-dichlorophenol using titanium dioxide deposited on fiber optics. The results showed that there is a linear relationship in the temperature range of 10-60 °C (Hofstadler et al., 1994). Fig. 4(d) shows the effect of photocatalyst dose and time on the dye removal efficiency. In this diagram, the dose of photocatalyst varied between 0.94 and 3.06 g/liter and the time between 43.68 and 206.32 min. In this graph, as in Fig. 4 (a), with the decrease in pH and the increase in time, the dye removal efficiency increased from 27.87% at 0.94 photocatalyst dose and time of 43.68 min to 33.78% dye removal in time of 206.32 min and dose 3.06 g/liter. Fig. 4(e) shows the effect of photocatalyst dose and temperature on dye removal efficiency. In this graph, the dose of photocatalyst varied between 0.94 and 3.06 g/liter and the temperature between 15.86 and 44.14 °C. In this graph, as in Fig. 4(c) with increasing temperature and 4(d)

with increasing photocatalyst dosage, the dye removal efficiency increased so that the dye removal reached from 32.06% at photocatalyst dose of 0.94 and temperature of 15.86 °C to 40.23% dye removal at temperature of 44.14 °C and photocatalyst dose of 3.06 g/liter. Fig. 4 (f) shows the effect of time and temperature on the dye removal efficiency. In this graph, the time varied between 43.68 and 286.32 min and the temperature between 15.86 and 44.14 °C. In this graph, as in Fig. 4(c) and (e), the dye removal efficiency increased with increasing temperature and 4(d) and process time, So that the removal of dye from 29.13% in time of 43.68 min and temperature of 15.86 °C reached to 38.56% at temperature of 44.14 °C and time of 206.32 min. Table 4 shows the optimal values predicted in the methyl orange dye removal model using the photocatalytic method. Based on Table 3, the efficiency of photocatalytic degradation of dye was obtained based on the results, 49.80% with a desirability value of 1. Finally, to confirm the validity of the predicted response, the experiment was repeated three times under the conditions proposed by the model. Based on the experimental results, the optimal conditions for the maximum photocatalytic degradation of methyl orange dye pollutant were obtained at the catalyst dose of 3 g/L, irradiation time of 148.34 min, pH=4 and reaction temperature of 44.12 °C.

**Table 4**
Optimum conditions and experimental results for photocatalytic degradation of methyl orange

| | | | **Variable** | | **Predicted value** | |
|---|---|---|---|---|---|---|
| Run | Dosage (g/L) | pH | Temperature (oC) | Time (min) | Dye removal (%) | Desirability value |
| 1 | 3 | 4 | 44.12 | 148.34 | 49.80 | 1 |
| 2 | 3 | 4 | 44.12 | 184.75 | 49.62 | 0.98 |
| 3 | 3 | 4 | 43.79 | 164.50 | 50.47 | 0.99 |

To survey the stability of the $Fe_2O_3$@ZnO photocatalyst, reuse experiments of the synthesized photocatalyst were performed and the results of the tests are shown in Fig. 5. A small amount of reduction in the removal efficiency of methyl orange was observed at the end of the second and third cycles. This decrease in dye removal percentage can be due to the accumulation of intermediate organic compounds produced during the photocatalytic process in the pores and on the surface of the photocatalyst, which has led to a decrease in the activity of the photocatalyst. The results of this investigation clearly show that the synthetic photocatalyst is stable and can be used for multiple purification cycles without losing the initial activity.

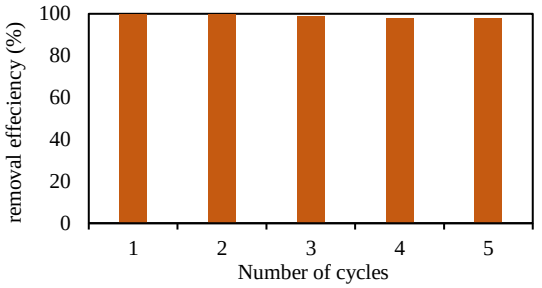



**Fig. 5.** Recycling rate of dye removal by $Fe_2O_3$@ZnO for photocatalytic degradation

## CONCLUSION

This research successfully demonstrates the effective removal of the dye methyl orange from aqueous solutions using a $Fe_2O_3$@ZnO core-shell nanocomposite as a photocatalyst. Through the application of the Response Surface Methodology (RSM) and Central Composite Design (CCD), the study optimized key operational parameters—catalyst dose, pH, temperature, and irradiation time—to achieve a maximum dye removal efficiency of 49.80%. The findings indicate that temperature and pH significantly influence the photocatalytic degradation process, with the optimal conditions identified as a catalyst dose of 3 g/L, pH 4, a temperature of 44.12 °C, and an irradiation time of 148.34 minutes. Furthermore, the structural analysis of the synthesized nanocomposite through SEM, XRD, and EDX confirmed its effective formation and characteristics. The recovery tests over five consecutive cycles showcased the robust reusability of the $Fe_2O_3$@ZnO photocatalyst, highlighting its potential for practical applications in treating dye-laden wastewater. Overall, the results suggest that the $Fe_2O_3$@ZnO nanoparticles not only possess high efficiency in removing dye pollutants but also represent a promising and sustainable approach for wastewater treatment in the textile and dyeing industries. This research contributes valuable insights into the development of effective strategies for mitigating environmental pollution caused by dye effluents.

## REFERENCES

[1] Al-Sayyed G, D'Oliveira JC, Pichat P. Semiconductor-sensitized photodegradation of 4-chlorophenol in water. J Photochem Photobiol A Chem. 1991;58:99-114.

[2] Alsukaibi AK. Various approaches for the detoxification of toxic dyes in wastewater. Processes. 2022;10:1968.

[3] Amini M, Younesi H. Biosorption of Cd (II), Ni (II) and Pb (II) from aqueous solution by dried biomass of Aspergillus niger: application of response surface methodology to the optimization of process parameters. Clean Soil Air Water. 2009;37:776-786.

[4] Batra V, Kaur I, Pathania D, Chaudhary V. Efficient dye degradation strategies using green synthesized

ZnO-based nanoplatforms: a review. Appl Surf Sci Adv. 2022;11:100314.
[5] Fox MA, Doan KE, Dulay MT. The effect of the "inert" support on relative photocatalytic activity in the oxidative decomposition of alcohols on irradiated titanium dioxide composites. Res Chem Intermed. 1994;20:711-721.
[6] Gallego-Ramírez C, Chica E, Rubio-Clemente A. Coupling of advanced oxidation technologies and biochar for the removal of dyes in water. Water. 2022;14:2531.
[7] Gaya UI, Abdullah AH, Hussein MZ, Zainal Z. Photocatalytic removal of 2,4,6-trichlorophenol from water exploiting commercial ZnO powder. Desalination. 2010;263:176-182.
[8] Giwa A, Yusuf A, Balogun HA, Sambudi NS, Bilad MR, Adeyemi I, et al. Recent advances in advanced oxidation processes for removal of contaminants from water: a comprehensive review. Process Saf Environ Prot. 2021;146:220-256.
[9] Gupta R, Eswar NK, Modak JM, Madras G. Ag and CuO impregnated on Fe doped ZnO for bacterial inactivation under visible light. Catal Today. 2018;300:71-80.
[10] Hofstadler K, Bauer R, Novalic S, Heisler G. New reactor design for photocatalytic wastewater treatment with TiO2 immobilized on fused-silica glass fibers: photomineralization of 4-chlorophenol. Environ Sci Technol. 1994;28:670-674.
[11] Islam T, Repon MR, Islam T, Sarwar Z, Rahman MM. Impact of textile dyes on health and ecosystem: a review of structure, causes, and potential solutions. Environ Sci Pollut Res. 2023;30:9207-9242.
[12] Ismail GA, Sakai H. Review on effect of different type of dyes on advanced oxidation processes (AOPs) for textile color removal. Chemosphere. 2022;291:132906.
[13] Khammar S, Bahramifar N, Younesi H. Optimization using the response surface methodology for adsorption of polychlorinated biphenyls (PCBs) from transformer oil by magnetic CMCD-Fe3O4@SiO2 nanoparticles. Mater Chem Phys. 2020;252:123195.
[14] Khammar S, Bahramifar N, Younesi H. Preparation and surface engineering of CM-β-CD functionalized Fe3O4@TiO2 nanoparticles for photocatalytic degradation of polychlorinated biphenyls (PCBs) from transformer oil. J Hazard Mater. 2020;394:122422.
[15] Peramune D, Manatunga DC, Dassanayake RS, Premalal V, Liyanage RN, Gunathilake C, et al. Recent advances in biopolymer-based advanced oxidation processes for dye removal applications: a review. Environ Res. 2022;215:114242.
[16] Preočanin T, Kallay N. Point of zero charge and surface charge density of TiO2 in aqueous electrolyte solution as obtained by potentiometric mass titration. Croat Chem Acta. 2006;79:95-106.
[17] Rahman M. A performance and energy evaluation of a dye drawn forward osmosis (FO) system for the textile industry [thesis]. Cape Town: Cape Peninsula Univ Technol; 2020.
[18] Shekoohiyan S, Rahmanian O, Alipour V, Chamack M, Rahmania A. Removal of Bisphenol A from water using Fe2O3/ZnO photocatalytic process in the presence of visible light. J Prev Med. 2020;7:22-35.
[19] Slama HB, Chenari Bouket A, Pourhassan Z, Alenezi FN, Silini A, Cherif-Silini H, et al. Diversity of synthetic dyes from textile industries, discharge impacts and treatment methods. Appl Sci. 2021;11:6255.
[20] Soleimani H, Sharafi K, Parian JA, Jaafari J, Ebrahimzadeh G. Acidic modification of natural stone for Remazol Black B dye adsorption from aqueous solution-central composite design (CCD) and response surface methodology (RSM). Heliyon. 2023;9:e17832.
[21] Song S, Fan J, He Z, Zhan L, Liu Z, Chen J, et al. Electrochemical degradation of azo dye CI Reactive Red 195 by anodic oxidation on Ti/SnO2–Sb/PbO2 electrodes. Electrochim Acta. 2010;55:3606-3613.
[22] Sushma C, Girish Kumar S. Advancements in the zinc oxide nanomaterials for efficient photocatalysis. Chem Pap. 2017;71:2023-2042.
[23] Taufik A, Saleh R. Synthesis of iron (II, III) oxide/zinc oxide/copper (II) oxide (Fe3O4/ZnO/CuO) nanocomposites and their photosonocatalytic property for organic dye removal. J Colloid Interface Sci. 2017;491:27-36.
[24] Wang KH, Hsieh YH, Ko RC, Chang CY. Photocatalytic degradation of wastewater from manufactured fiber by titanium dioxide suspensions in aqueous solution. Environ Int. 1999;25:671-676.
[25] Yashni G, Al-Gheethi A, Mohamed R, Hossain MS, Kamil AF, Abirama Shanmugan V. Photocatalysis of xenobiotic organic compounds in greywater using zinc oxide nanoparticles: a critical review. Water Environ J. 2021;35:190-217.
[26] Zeltner W Jr. Supported titania for photodegradation. Chemtech. 1993;23:21.